Influence of pore size distribution on Pt dispersion in Pt-Sn/Al$_2$O$_3$ reforming catalyst

L.D. Sharma[*], Manoj Kumar, A.K. Saxena, Mool Chand, J.K. Gupta

Indian Institute of Petroleum, Dehradun 248005, India

Abstract

Pt-Sn/Al$_2$O$_3$ catalysts; Pt (0.35 wt.%), Sn (0.42 wt.%) and chlorine ($\sim$1.0 wt.%) were prepared by incipient wetness impregnation and characterized by nitrogen adsorption–desorption, NH$_3$ adsorption microcalorimetry and H$_2$–O$_2$ titrations. In catalysts with almost similar values of S_{BET} (170–180 m^2 g^{-1}), total acidity (0.32–0.36 mmol NH$_3$ g^{-1}), a significant variation in Pt dispersion was observed with the difference in meso pore size distribution in 20–100 Å diameter range. As the vol.% in 20–100 Å range is increased from 18 to 63%, the Pt dispersion increased from 57 to 81%. A greater abundance of relatively narrow meso pores (20–100 Å diameter) facilitate the fine dispersion of Pt moieties on the alumina surface. At least, a 30% fraction of the total pore volume should lie in 20–100 Å pores in order to obtain a reasonably good Pt dispersion ($\sim$75%). Although, a further increase of volume in these pores from 30 to 60% improves the Pt dispersion, but decreases the total pore volume presumably due to a sharp decline in larger pores (100–200 Å) which contribute more towards the pore volume.
© 2002 Published by Elsevier Science B.V.

Keywords: Pt-Sn/Al$_2$O$_3$; Pore size distribution; Pt dispersion; Reforming catalyst

1. Introduction

One of the essential requirements of a bimetallic reforming catalyst is the efficient dispersion of the active metallic species on a porous support. Equally important is the maintenance of that high area during extended periods of the process operation. Metal particle dimensions and high dispersion of Pt impart superior activity and selectivity for a number of structure sensitive reactions [1,2]. Since, the catalytic phenomenon occurs in the internal surface of the solid, lying within the pores, optimization of pore size becomes important for the mass transfer and diffusion of the reactants to the active sites. The pores are not only the paths for the reactants and products but, also influence the incorporation of active metals during preparation of the catalyst and coke deposition during deactivation. With smaller pores (micropores), the activity of catalyst becomes limited to diffusion while with wider pores (macropores), less active surface area is available. Morphological characteristics like surface area, pore volume and pore size distribution have to meet the required specifications for a longer catalyst life [3].

Alumina has been a traditional support for noble metal catalysts to suit a wide variety of catalytic applications like catalytic reforming, hydrotreating, oxidation and exhaust emission. The pore size can be controlled to precise narrow ranges for specific requirements of feed molecules by adopting the methods of preparation of the gel or by addition of pore

---

* Corresponding author.
E-mail address: ldsharma@iip.res.in (L.D. Sharma).

regulating agents [4,5]. Pt-Sn/Al$_2$O$_3$ is used in continuous catalyst regeneration (CCR) mode in petroleum industry for naphtha reforming and aromatic production [6]. The catalyst is used under severe conditions of low hydrogen pressure where it gets deactivated very fast and has to undergo several regenerations during its life. Selection of a suitable alumina support with critically controlled textural characteristics thus, becomes necessary in order to obtain an active acidic bimetallic dual functional reforming catalyst with high metal dispersion. This work, is aimed to study the effect of meso pores of alumina on Pt dispersion in Pt-Sn/Al$_2$O$_3$ catalyst.

2. Experimental

The catalysts were prepared on three commercial γ-alumina spheres (Condia Chemie) of different pore volume and pore size distribution (Table 1). The γ-alumina supports were immersed in an excess solution of N/15 hydrochloric acid for 16 h for optimum chlorine uptake(target Cl ~1 wt.%). Simultaneous impregnation of chloroplatinic acid and stannous chloride salt solutions in acetone medium was then carried out using incipient wetness technique. A red colour of the mixture indicates the formation of platinum–tin complex. The catalysts were calcined at 550 °C in air. The three catalysts prepared by the same impregnation method were designated as Pt-Sn-Al$_2$O$_3$-A, B and C; and contained 0.35 wt.% Pt, 0.42 wt.% Sn and 1.02, 0.97 and 0.90 wt.% Cl, respectively.

Surface area and pore size analyzer (ASAP 2010, Micromeritics, USA) was used to study the N$_2$ adsorption–desorption isotherm at −195 °C. The meso pore size distribution was computed from the desorption branch using BJH method [7]. The total pore volume was taken at the saturation of mesopores around $P/P_0 = 0.99$. Microporosity was determined from the t-plots [8,9].

The acidity and acid strength distribution were measured using a Tian-calvet type microcalorimeter (model C80, Setaram, France), connected to a volumetric vacuum adsorption unit for catalysts treatment and probe molecule delivery. Microcalorimetry of NH$_3$ adsorption was carried out through the measurement of differential heats evolved upon adsorption of small quantities of NH$_3$ on the catalyst until the surface saturation. Such measurements, over a range of surface coverage yield quantitative information about the acid strength distribution. The calorimetric measurements of NH$_3$ adsorption were made at 175 °C to limit physisorption.

The dispersion of platinum was measured by carrying out oxygen titrations using a dynamic pulse flow technique (Pulse Chemisorb 2700, Micromeritics). The details of the method have been described elsewhere [10]. The catalyst (1 g) after pretreatment at 500 °C for 2 h in the flow of helium carrier gas was reduced at 500 °C for 3 h in H$_2$ flow (50 cm^3/min) and was then cooled to room temperature (RT) in the flow of hydrogen and flushed with carrier gas. The first oxygen titration (OT1) was then carried out at RT. The catalyst after OT1 was treated with H$_2$ gas at RT for half an hour, flushed with helium and then second oxygen titration OT2 was conducted. The Pt dispersion was determined from OT2.

3. Results and discussion

The physico-chemical characterization data has been displayed in Table 1. Nitrogen adsorption–desorption isotherms (Fig. 1.) for the catalysts studied,

Table 1
Textural properties of Pt-Sn-Al$_2$O$_3$ catalysts[a]

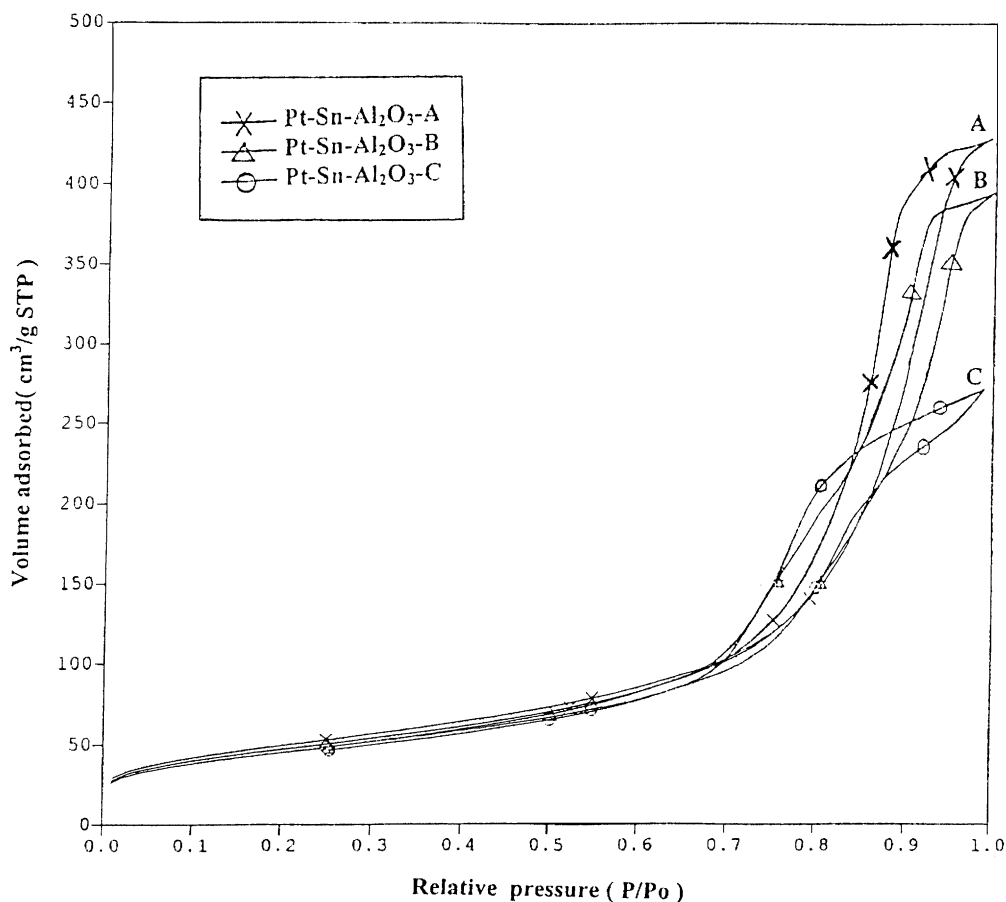| Catalysts	S_{BET} (m^2/g)	S_t (m^2/g)	Total pore volume (cm^3/g)	Micro pore volume (cm^3/g)	Vol.% in pores of diameter (Å)					Pore maxima (Å)	Dispersion D(Pt) (%)
					<20	20–100	100–200	200–500	500–2000		
Pt-Sn-Al$_2$O$_3$-A	179	168	0.66	0.0034	0.52	18.14	73.28	7.43	0.63	150	57
Pt-Sn-Al$_2$O$_3$-B	171	162	0.61	0.0024	0.39	32.40	42.96	23.39	0.86	95, 195 (Bimodal)	76
Pt-Sn-Al$_2$O$_3$-C	168	158	0.42	0.0031	0.74	63.01	27.69	6.75	1.82	90	81

[a] S_t: t-area.

Fig. 1. Nitrogen adsorption–desorption isotherms of Pt-Sn-Al$_2$O$_3$ catalysts.

are of type IV [8] exhibiting H1 hysteresis loops [8,11] characteristic of solids consisting of particles forming cylindrical channels of mesopore range. The closure of hysteresis loop at $P/P_0 > 0.40$ is indicative of the absence of micropores and the formation of well-defined mesoporous texture. The parallel path shape of the hysteresis loop clearly indicates the presence of cylindrical pores.

The *t*-plots (Fig. 2.) with small *y*-intercept indicate very little micropore volume (Table 1) and the *t*-area (S_t) derived therefrom, are in good agreement ($\pm 5\%$) with S_{BET}, further supporting the absence of microporosity and confirming the mesoporous texture of these catalysts. An upward deviation observed in *t*-plots corresponds to capillary condensation due to adsorbate–adsorbate interaction. The lower linear

portion of the *t*-plot correspond to a reversible mono-multilayer adsorption–desorption in the mesopores before the capillary condensation occurs. The major contribution to pore-volume seems to be due to the pores in the range 20–200 Å diameter. The pores in the range 200–500 Å are less than 10% in catalysts A and C, but are higher in catalyst B ($\sim$23%) probably due to its bimodal pore size distribution (pore maxima at 95 and 195 Å). It has been observed that, while the vol.% in pores of 20–100 Å increases from 18 to 63% from catalysts A to C, a decreasing trend was observed in the 100–200 Å pore range. Although, this has not reflected much in S_{BET} but a marked decrease in total pore volume has occurred in catalyst C.

The microcalorimetric curves of differential heats of adsorption of NH$_3$ are shown in Fig. 3. The differential
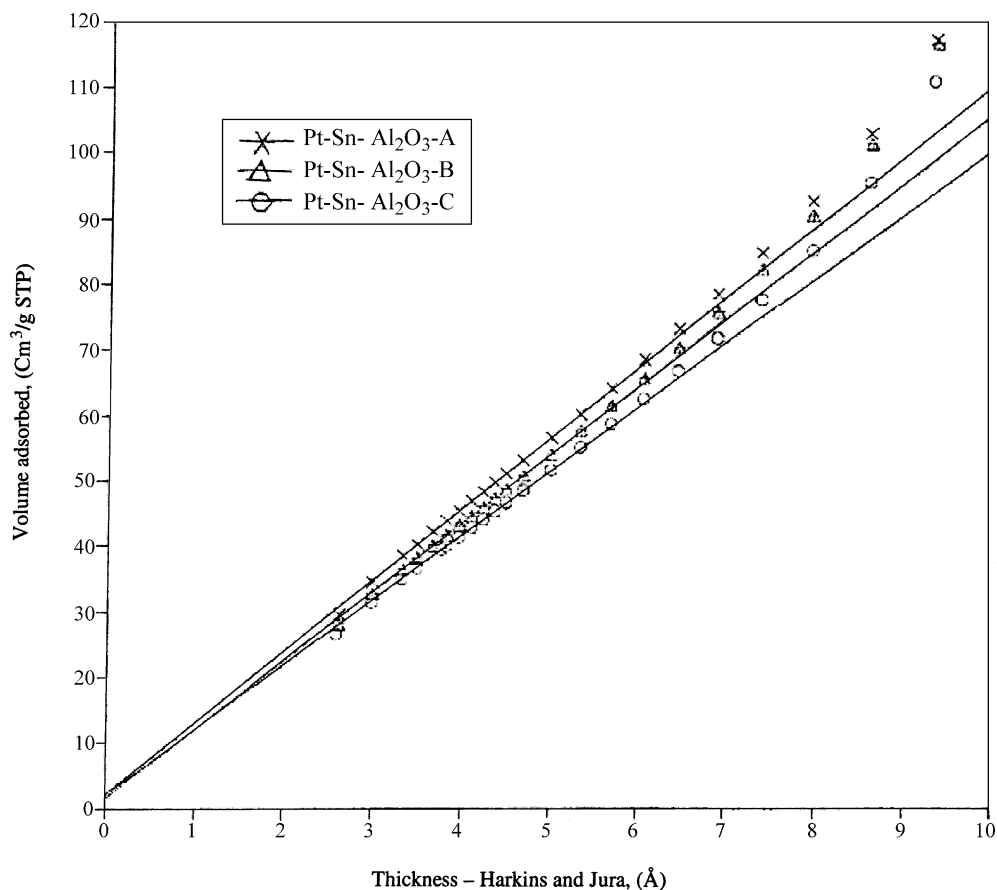
Fig. 2. *t*-Plots of Pt-Sn-Al$_2$O$_3$ catalysts.

heats of adsorption (kJ/mol) versus surface coverage (mmol/g) are stepwise curves indicating the energetic heterogeneity of acid sites and a wide distribution of acid strength [12]. The initial heat of NH$_3$ adsorption is slightly higher in catalysts A and B as compared to catalyst C due to the presence of relatively higher

strength of strong acid sites. All the three catalysts exhibits almost similar acid strength distribution as shown in Table 2. The data is derived from Fig. 3 and is based on the acidity scale of differential heats of NH$_3$ adsorption viz. strong: >100 kJ/mol; medium: 100–80 kJ/mol; and weak <80 kJ/mol.

Table 2
Oxygen titration/Pt dispersion and acidity/acid strength distribution of Pt-Sn-Al$_2$O$_3$ catalysts

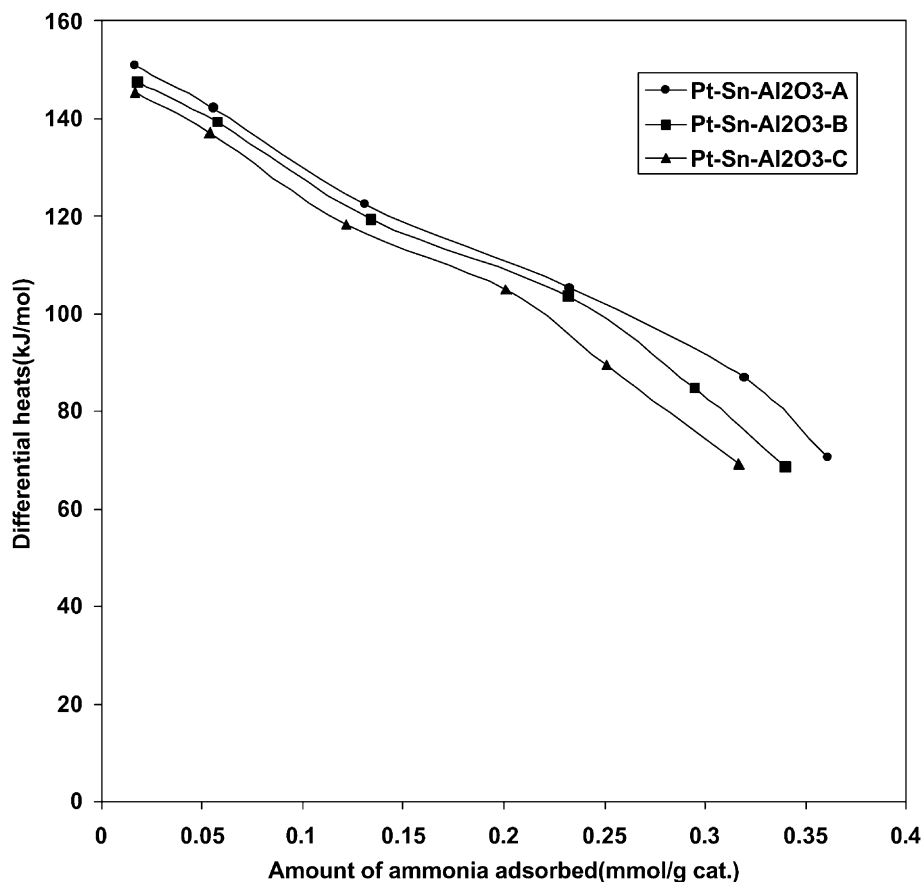| Catalysts	O$_2$ uptake STP (µ mol/g catalyst)		Dispersion[a] D(Pt) (%)	Total acidity (mmol NH$_3$/g catalyst)	Acid strength distribution (mmol NH$_3$/g catalyst)		
	OT1	OT2			Strong	Medium	Weak
Pt-Sn-Al$_2$O$_3$-A	10.50	6.43	57	0.36	0.25	0.09	0.02
Pt-Sn-Al$_2$O$_3$-B	15.52	8.62	76	0.34	0.24	0.08	0.02
Pt-Sn-Al$_2$O$_3$-C	12.71	9.51	81	0.32	0.22	0.07	0.03

[a] Calculated from OT2.

Fig. 3. Differential heats versus ammonia coverage of Pt-Sn-Al$_2$O$_3$ catalysts.

Modification of alumina support with chlorine influences the cracking activity and metal/acid balance required for dehydrocyclization and isomerization [13]. In commercial bimetallic Pt-Re, Pt-Sn/Al$_2$O$_3$ reforming catalysts an optimum 1 wt.% Cl is maintained during the process to provide a good metal/acid function for selective aromatic production [14]. On gradually increasing the chlorine content in alumina, the concentration of strong acid sites increases till it becomes constant at around 1 wt.% chlorine [15]. The chlorine in presence of oxygen during calcinations and regeneration (coke burning)/oxychlorination (redispersion) enhances the formation of a mobile platinum oxychloride, (Pt^{IV}O$_x$Cl$_y$)s species which distributes uniformly on and interacts strongly with the support resulting in a stable and high Pt dispersion [16,17].

The surface area of the alumina support and its acidity could play a vital role in governing the dispersion of Pt. It has been reported that alumina should have surface area >150 m^2 g^{-1} in order to achieve good dispersion of metal on support [18]. In all of our catalysts, the surface area and acidity values were almost same but we have observed that the dispersion of Pt is changing with pore size in 20–100 Å diameter range. In Pt-Sn-Al$_2$O$_3$-A where the vol.% in pores of diameter 20–100 Å is 18%, the dispersion of Pt is as low as 57% only. As % the volume in 20–100 Å range increases to 32% in catalyst B, the Pt dispersion has increased to 76%. In catalyst C the 20–100 pores have gone up to 63%, the dispersion has also increased to 81%. The effect can be seen clearly in Fig. 4. It may be pointed out that at least a platinum dispersion of 70% is desired
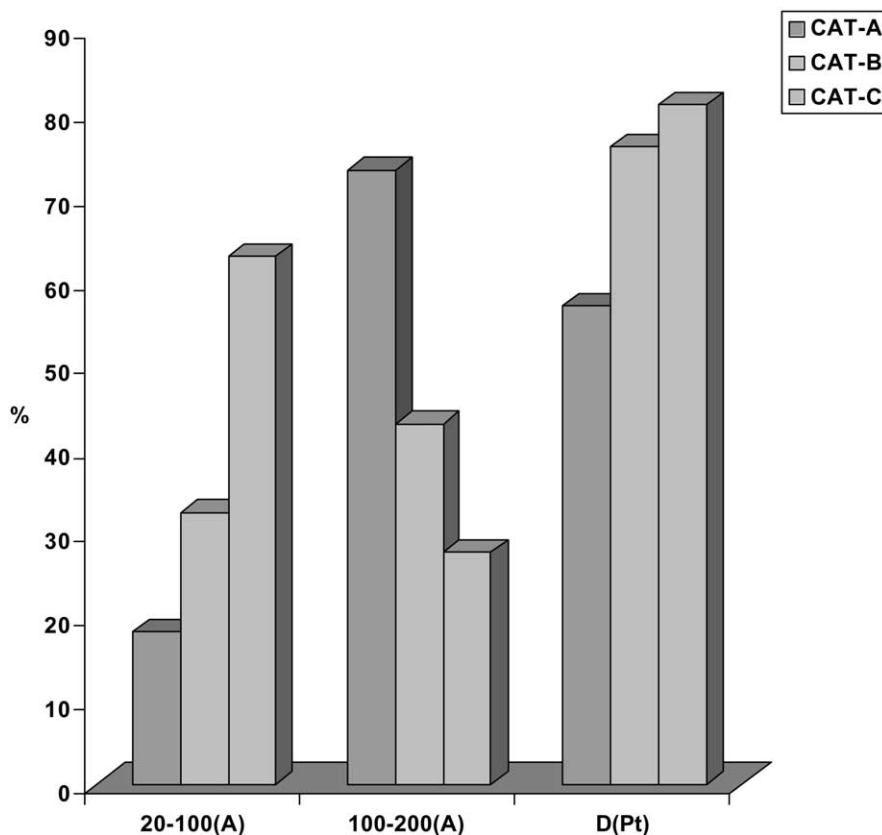
Fig. 4. Dispersion D(Pt) versus pore size distribution of Pt-Sn-Al$_2$O$_3$ catalysts.

for an efficient commercial Pt-Re or Pt-Sn/Al$_2$O$_3$ bimetallic reforming catalysts selective for aromatic production, provided, the other specifications of textural characteristics are met. In catalyst C, although, the dispersion is fairly good (81%) but the total pore volume has decreased considerably, probably due to the presence of fairly large proportions of 20–100 diameter pores (63%) and a relatively less abundance of large pores 100–200 range, as the latter contribute more towards the pore volume. A drastic decrease in the total pore volume would result in an increase in the apparent bulk density of the Pt-Sn/Al$_2$O$_3$ spheres which could make it unsuitable for moving bed operations. Small pores ($\sim$100 Å) are mainly controlled by the size of the alumina crystallite as these originate from the dimensions and shape of spaces between the particles of alumina (intra particle void spaces). On the other hand, large pores (macropores) generally

originate from inter particle spaces. Smaller metal particles are considered, to a great extent, in contact with supports of narrow channel porous texture. For example, when metal clusters are present inside the zeolite channels they have larger surface in contact with support. For this reason, metal support interactions are larger in zeolites than on alumina carriers [19]. Zeolites (Pt-KL) are now being explored as an alternatives to the conventional alumina carriers for catalytic applications like aromatization because, a very small metal particle ($<$10 Å) can be created uniformly inside fine zeolite channels [20]. But these are yet to be commercially exploited.

It is not easy to design an alumina supported catalyst with a very precise pore size [21]. It can be stated that the meso pores in 20–100 Å diameter range are of paramount importance in Pt-Sn/Al$_2$O$_3$ CCR catalyst and at least a 30% of pore volume should lie in this

range, in order to achieve a reasonably good Pt dispersion (>70%). A further increase of pores in 20–100 Å range has beneficial effect on dispersion, but the total pore volume is deteriorated. A compromise has to be made between pore volume, pore size distribution and metal dispersion.

References

[1] B.C. Gates, Chem. Rev. 95 (1995) 511.

[2] J.J. Burton, Catal. Rev. 9 (1974) 209.

[3] J.C. Plumail, Y. Jacquin, G. Martino, H. Toulhoat, Preprint, Div. Petrol. Chem. A.C.S. 28 (1983) 562.

[4] R. Snel, Appl. Catal. 11 (1984) 271.

[5] D.L. Trimm, A. Stanislaus, Appl. Catal. 21 (1986) 215.

[6] R.E. Rausch, US Patent, 3, 745, 112, (1973).

[7] E.P. Barret, L.G. Joyner, P.H. Halenda, J. Am. Chem. Soc. 73 (1951) 373.

[8] S.J. Gregg, K.S.W. Sing, Adsorption, Surface Area and Porosity, Academic Press, London, 1982.

[9] M.F.L. Johnson, J. Catal. 52 (1978) 425.

[10] L.D. Sharma, M. Kumar, A.K. Saxena, D.S. Rawat, T.S.R. Prasada Rao, Appl. Catal. A 168 (1998) 251.

[11] K.S.W. Sing, D.H. Everett, R.A.W. Haul, L. Moscou, R.A. Pierotti, J. Rouquerol, T. Siemieniewska, Pure Appl. Chem. 57 (1985) 603.

[12] B.E. Spiewak, B.E. Handy, S.B. Sharma, J.A. Dumesic, Catal. Lett. 23 (1994) 207.

[13] R.J. Verderone, C.L. Pieck, M.R. Sad, J.M. Parera, Appl. Catal. 21 (1986) 239.

[14] C.G. Michel, W.E. Bambrick, R.H. Ebel, Fuel Process. Tech. 35 (1993) 159.

[15] S.R. Bajaj, P. Pal, J.K. Gupta, L.D. Sharma, G. Muralidhar, T.S.R. Prasada Rao, Stud. Surf. Sci. Catal. 113 (1998) 365.

[16] H. Lieske, J. Volter, J. Catal. 90 (1984) 96.

[17] J. Basset, C. Naccache, M. Mathier, M. Prettre, J. Chem. Phys. 66 (1969) 1522.

[18] V. Eskinazi, Appl. Catal. 4 (1982) 37.

[19] M. Vaarkamp, F.S. Modica, J.T. Miller, D.C. Koningsberger, J. Catal. 144 (1993) 611.

[20] G. Jacobs, W.E. Alvarez, D.E. Resasco, Appl. Catal. A Gen. 206 (2001) 267.

[21] J. Walendziewski, J. Trawczynski, Appl. Catal. A Gen. 96 (1993) 163.